Polymer Bulletin 56, 179–191 (2006)
DOI 10.1007/s00289-005-0452-8

Polymer Bulletin

Crystallization Behaviors of amino-terminated polyurethane (ATPU)-grafted polypropylene

Yu Zhang[1], Xianlong Jiang[1], Yong Guan[1], Anna Zheng[1] (✉), Huining Xiao[2]

[1] (School of Material Science and Engineering, East China University of Science and Technology, Key Laboratory for Ultrafine Material of the Ministry of Education ECUST, Shanghai, China, 200237)
[2] (Department of Chemical Engineering, University of New Brunswick, P.O. Box 4400, Fredericton, N.B. E3B 5A3 Canada)

Fax: 086-021-6425-2744; Email: zan@ecust.edu.cn

Received: 14 July 2005 / Revised version: 31 August 2005 / Accepted: 26 September 2005
Published online: 11 January 2006 –

Abstract

A melt-grafting approach was employed to prepare a novel functional polypropylene(FPP)—amino-terminated polyurethane grafted polypropylene (PP-g-ATPU). The crystallization behaviors of PP and PP/FPP blends were characterized using differential scanning calorimetry (DSC), wide angle X-ray scattering (WAXS) and polarized optical microscopy (POM). The effects of FPP composition on crystallization behavior, crystal transformation, and morphology of PP/FPP crystalline were investigated. The results showed that at a low dosage (< 2.0wt%) ATPU acted as a heterogeneous nucleation agent during the crystallization of PP/FPP blends. However, when the content of ATPU reached 2.0wt% or higher, ATPU deteriorated the crystallization of PP or PP/FPP blends. The crystallite size decreased and the number of crystallites increased as the ATPU content increased. The Avrami analysis was adopted to describe the isothermal crystallization process. The difference in the exponent n between PP and PP/FPP suggested that the isothermal crystallization kinetics of PP/FPP blends followed a three-dimensional growth via heterogeneous nucleation. In terms of the half-time of the crystallization, $t_{1/2}$, the crystallization rate of functional PP blends was faster than that of PP homopolymer at a given crystallization temperature.

Keywords: Crystallization; ATPU; grafted; polypropylene; DSC; WAXS

Introduction

Since isotactic polypropylene (iPP) was industrialized in 1950's, extensive research has been conducted on iPP modification and applications due to its relatively low cost and versatile properties. However, the high crystallinity and non-polarity of iPP lead to lower impact strength, poor compatibility and adhesion towards other materials;

thus constraining its applications. To improve it's the performance of iPP, a number of modifying approaches have been explored in the past, typically copolymerization and grafting [1].

Physical properties of polymeric materials strongly depend on their microstructure and crystallinity, thus studies on the crystallization behaviors and morphology as well as their relations with the mechanical properties of modified PP have been carried out extensively by many researchers[2-11]. Particular attention has been paid to the crystallization behavior of modified PP via grafting maleic anhydride[12-17]. Qi H.J.[18] prepared PP-g-MAH by reactive-processing.

The isothermal crystallization kinetics of the PP-g-MAH polymers was investigated by DSC. The results showed a remarkable decrease at the rate of crystallization of the grafted polypropylene compared to PP. The crystallization rate of PP-g-MAH and Avrimi exponent *n*, decreased with the temperature increasing. Kilwon Cho [12] studied the crystallization behavior of polypropylene and maleated polypropylene blends. Studies on the isothermal crystallization kinetics confirm that there is a correlation between the crystallization rate and the resulting morphologies. J. He et. al.[13] studied crystallization kinetics of maleic anhydride grafted polypropylene. The crystallization kinetics was investigated under isothermal and non-isothermal conditions. Under both conditions, the introduction of pendant groups along the PP chains increased the crystallization rate and did not influence the crystallization type.

There are several reports about the crystallization behaviors of PP-g-AA (Acrylic acid) and PP-g-GMA (Glycidyl methacrylate). Zhang X. M.[19], Yang X. B.[20] studied crystallization of PP-g-AA. They found that PP-g-AA had different crystallization mode from that of PP. Yin Z.H.[21] studied the isothermal crystallization of PP-g-GMA copolymer, and results showed that the number of effective nuclei in grafted samples was estimated to be 10^2-10^3 times larger than that in PP. The overall crystallization rates of PP were lower than that of grafted samples. The monomer grafted onto PP acts as a heterogeneous nucleator in the polymer crystallization process.

In this work, we focused on grafting an ATPU (Amino-terminated polyurethane) onto PP via a melt-grafting method. The ATPU was synthesized by reacting toluene-2,4-diisocyanate (TDI) with polyethylene glycol (PEG) and diamine, using dibutyltin dilaurate (DBTDL) as a catalyst. The ratio of soft segment and hard segment, and the molecular weight of ATPU are adjustable, which facilitates the studies of the structure-property relationship. GMA (Glycidyl methacrylate) was used as a coupling agent to enhance the bonding between PP and ATPU. The crystallization behaviors of PP/modified PP blends was investigated using differential scanning calorimetry (DSC), wide angle X-ray scattering (WAXS) and polarized optical microscopy (POM). The crystallization kinetics of the samples was studied by spectral depolarization.

Experimental

Materials

The isotactic PP (Y1600 in pellet, Shanghai Petrochemical Industrial Co., Ltd., P.R. China) was used as received. ATPU was self-prepared (M_n=3000), and the reaction is shown in Scheme 1. α,α-Bis (tert-butylperoxy) diisopropyl benzene (BIPB) (Trump Chemical Corp. Wuxi, Jiangsu, China), a free-radical initiator, was used as received.

ATPU synthesis consists of two polymerization reaction as shown in the Scheme 1. In the first reaction, polyether polyols react with an excess of di-isocyanate to form pre-polymers with terminated isocyanate groups; and the second step reaction is the chain extension reaction with diamines, the last product is amino-terminated polyurethane, which will be grafted on the PP backbone.

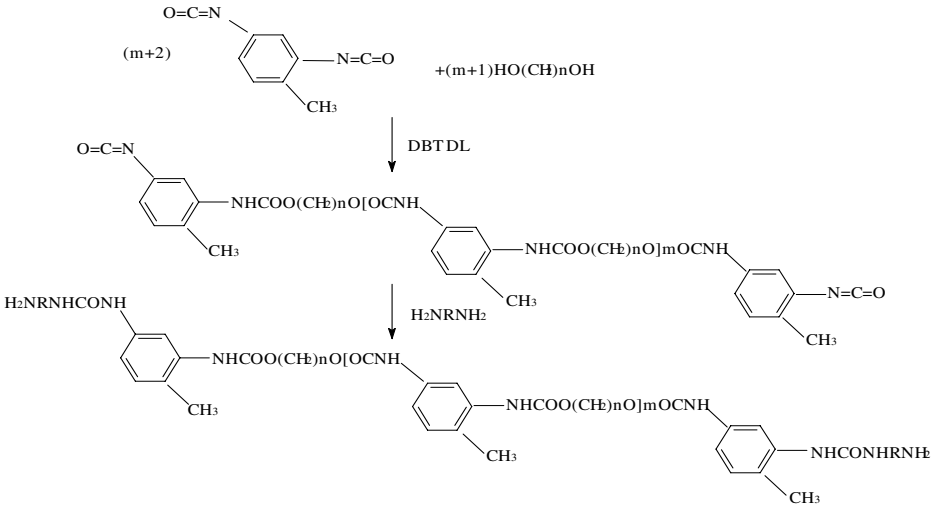

Scheme 1 The synthesis of ATPU

PP-g-ATPU (called FPP) was prepared by melt-grafting. About 20wt% of ATPU on FPP was added. The FPP was blended with PP in a twin-screw extruder (SHL-35, Shanghai 4th Chemical Machine Factory, Shanghai, P.R. China). Before being extruded, FPP and PP were dried at 80°C for over 4 h. The mixtures of FPP and PP at different ratios were extruded at 180°C under a screw rotating speed of 90 rpm, PP/ATPU blends also were prepared in the twin-screw extruder at 180°C. The extruded strands were cooled and then granulated.

Crystal analysis

The crystallization behaviors were investigated using a differential scanning calorimeter (DSC, NETSCH DSC 200PC). All samples were heated to 220°C at a rate of 20°C/min and held in the molten state for 5 min. to eliminate the influence of thermal history. The samples were cooled to room temperature at a rate of 10°C/min and held for 5min, followed by reheating to 220°C for the second heating run at a rate of 10°C/min. Both melting and crystallization parameters were obtained from the heating and cooling scans. All operations were carried out under a nitrogen environment.

In isothermal crystallization experiments, the samples were studied by spectral depolarization with a crystallization speedometer(GJY-III type, Donghua University, Shanghai, P.R.China). During the process of the crystallization, the polymer sample placed between two orthogonal polarizers, the intensity of depolarized light will increase proportionally with the crystallinity of the sample.

WAXS were performed on a Rigaku WAXS diffractometer (Japan), at 40kV and 35mA using CuK α-radiation with a wavelength of 1.541 angstrom as the X-ray source. Samples were scanned in the 2θ range of 4 to 31°. The samples for WAXD measurement were prepared in film by compression molding at 180°C and 5 MPa.

Kinetics of crystallization

The Avrami [22,23] equation has been proposed to analyze the isothermal crystallization of polymer:

$$1 - C = \exp(-Kt^n) \tag{1}$$

where n is the Avrami exponent, K, the crystallization rate constant and C is the relative crystallinity at time t. The crystallization half-time, $t_{1/2}$, defined as the time to a relative crystallinity of 50%, can be obtained:

$$t_{1/2} = (\frac{\ln 2}{K})^{1/n} \tag{2}$$

If the variation of the intensity of depolarized light at time t is $I_t - I_0$, the overall variety of the intensity of depolarized light is $I_\infty - I_0$, and C at time t can be represented as follows:

$$C = \frac{I_t - I_0}{I_\infty - I_0} \tag{3}$$

The Avrami equation can be rearranged as follows:

$$\frac{I_\infty - I_t}{I_\infty - I_0} = \exp(-Kt^n) \tag{4}$$

Equation (4) can further be expressed in a logarithmic form:

$$\lg[-\ln(\frac{I_\infty - I_t}{I_\infty - I_0})] = n \lg t + \lg K \tag{5}$$

By plotting the left side in the equation vs. lg$t$, we can get a straight line. The n (the slope of the straight line) and lg$K$ (the intersection) values can be calculated.

Results and Discussion

Preparation of PP-g-ATPU

Figure 1 shows the IR spectra of PP and FPP which were previously purified by SOXHLET extractor with acetone. In contrast to PP, the characteristic bands of carbonyl group C=O and imine group N-H of urethane at 1712 cm^{-1} and 3340 cm^{-1} respectively are observed in FPP samples. This demonstrated that ATPU was grafted on the PP backbone.

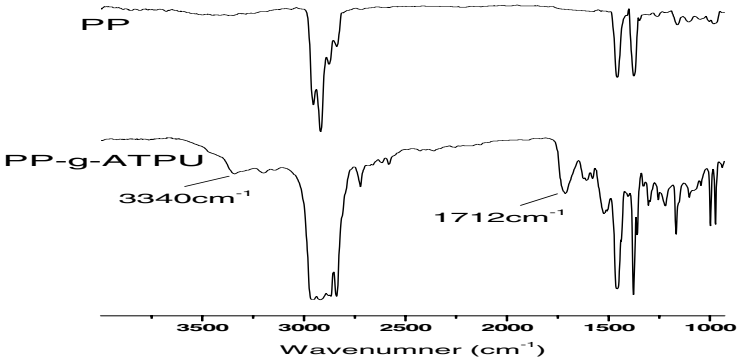

Figure 1 FTIR spectra of PP and PP-g-ATPU (FPP)

Figure 2 is the ^{13}C-NMR spectroscopy of PP-g-ATPU, the signal at approximately 70.0 ppm is methylene (-CH_2) connected with oxygen(O). NHCOO characteristic band appears in 164ppm, and δ=111ppm is the characteristic band of methylene(-CH_2) in diamine. So it is proved that the sample is PP-g-ATPU.

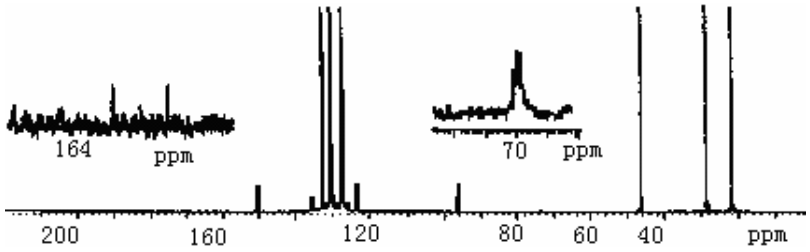

Figure 2 ^{13}C-NMR spectroscopy of PP-g-ATPU (FPP)

Isothermal crystallization

The Avrami plots obtained at various temperatures for pure PP are illustrated in Figure 3. Similar trends are shown for PP/FPP blends. There are good linearities of *lg[-ln(1-C)]* versus *lgt* in a wide relative crystallinity range (2-90%). It is clear that the

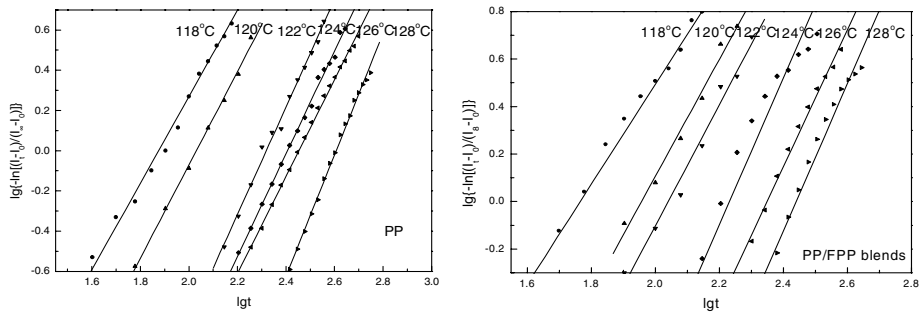

(a) PP (b) 90/10 PP/FPP

Figure 3 Avrami plots for isothermal crystallization of pure PP and PP/FPP at various crystallization temperature

Avrami equation is effective for analyzing the experimental data of the isothermal crystallization kinetics. The values of $K(t)$, n, and $t_{1/2}$, obtained from Figure 4, are listed in Table 1. As can be seen, $t_{1/2}$ of all samples increases with increasing crystallization temperature, while PP has the lowest $t_{1/2}$ at 118°C under experimental conditions. Depending on the mechanism of nucleation and crystal growth, n should have different integer values. But the non-integer values of the Avrami exponent were obtained for all the samples from experimental data, ranging from 1.6 to 2.2 and 2.5 to 3.0 at the crystallization temperature, 118°C and 128°C, respectively. The deviation is likely attributed to secondary crystallization processes, complex nucleation modes and

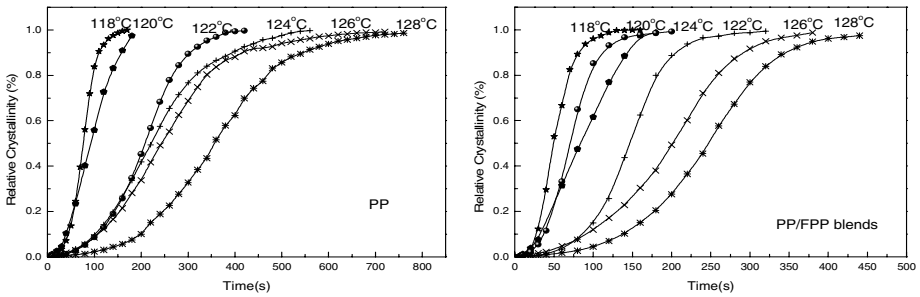

(a) PP (b) 90/10 PP/FPP

Figure 4 Relative crystallinity as a function time in isothermal crystallization

Table 1 The various parameters of samples from the Avrami equation

Samples (content of ATPU wt%)	T(°C)	n	lgK	$t_{1/2}$(s)
0(PP)	118	2.15	-4.04	76
	120	2.32	-4.71	103
	122	2.67	-5.91	242
	124	2.55	-6.14	352
	126	2.41	-6.19	441
	128	3.02	-7.87	503
0.5	118	1.62	-2.66	48
	120	1.89	-3.69	93
	122	2.09	-4.37	121
	124	2.56	-5.76	150
	126	2.62	-6.11	218
	128	2.88	-6.69	323
1.0	118	1.87	-3.80	37
	120	2.13	-4.41	81
	122	2.44	-5.04	92
	124	2.62	-5.95	144
	126	2.58	-6.01	189
	128	2.96	-7.57	306
1.5	118	1.99	-3.38	35
	120	2.57	-5.20	56
	122	2.63	-5.40	87
	124	2.60	-5.66	128
	126	2.89	-6.70	178
	128	2.78	-6.69	219

the change in material density. Moreover, some experimental errors introduced in the determination of the zero point of crystallization also led to non-integer value of *n*.
The $t_{1/2}$ values obtained from the experiments are also listed in Table1.They are consistent with those calculated from equation (2), indicating the validity of the Avrami equation in this study.
We analyzed the rate of crystallization, expressed by reciprocal half-times in terms of Hoffman's theory. Accordingly, the rate of crystallization, at which crystallinity develops from the melts, follows an Arrhenius-like relationship. The corresponding activation energy comprises of two contributions, one from the transport of the chain molecules towards the growing nuclei and another from nucleation. Since it is difficult to separate these two contributions precisely, we cast the equation here [24, 25]:

$$\ln\left(1/t_{1/2}\right) = A - B_k\,(T_m^0)^k\,/[\,T_c\left(\Delta T\right)^k\,] \qquad (6)$$

Where T_m^0 represents the equilibrium melting temperature (T_m^0 =481.15K); $\Delta T = T_m^0 - T_c$, the undercooling of the system; $K(K$=1,2) represents different crystallization model parameter, and A is a constant; B_K depends on the free energy of interface (б) and exothermic crystallization (ΔH_m^0):

$$B_k \infty (\sigma)^{k+1}\,/(\Delta \mathrm{H}_m^0)^k \qquad (7)$$

From Table 1, plots of $\ln\left(1/t_{1/2}\right)$ versus $(T_m^0)^k\,/[T_c\left(\Delta T\right)^k\,]$ should give straight lines with slope B_K (when k=1, 2, $\mathrm{B_{k1}}$ and $\mathrm{B_{k2}}$ were obtained). The relevant quantities, calculated from the slopes, are listed in Table 2. It is worth mentioning that the coefficient B_K of PP is higher than that of PP/FPP blends. This is due to the fact that the blends have lower nucleation free energy and nucleate readily.

Table 2 The value of B_k for PP and PP/FPP blends

Samples (content of ATPU wt%)	$\mathrm{B_{k1}}(\times 10^3)$	$\mathrm{B_{k2}}(\times 10^2)$
0	1.53	1.17
0.5	1.45	1.12
1.0	1.44	1.11
1.5	1.40	1.08

Melting and crystallization characteristics of PP and PP/FPP blends

The results of DSC heating and cooling scans for PP and PP/FPP blends are shown in Figure 5(a) and (b) respectively. It is evident that there is an endothermic melting peak in all the heating scans and there is a distinct exothermic crystallization peak in all the cooling scans. The corresponding parameters for melting and crystallization obtained from heating and cooling scans for all samples are presented in Tables 3 and 4. It is demonstrated that there is little difference between PP and PP/FPP in their onset temperature of melting ($\mathrm{T_{onset}}$) and $\mathrm{T_m}$. $\mathrm{T_{onset}}$ and melting peak width($\Delta \mathrm{T_m}$) are related to the least stability and distribution of crystallites, respectively. $\mathrm{T_{onset}}$, $\mathrm{T_m}$ and $\Delta \mathrm{H_f}$ of PP/FPP are lower than those of PP; whereas $\Delta \mathrm{T_m}$ of FPP is broader than that of PP at a low content of ATPU (<1.5wt%). The degree of crystallinity X was calculated in terms of the ratio of the melting enthalpies: $X=\Delta H/\Delta H_0$, where ΔH_0 is the melting

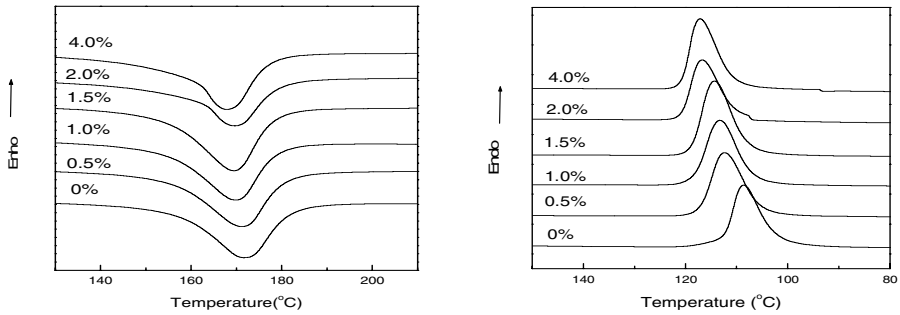

(a) heating scans (b) cooling scans

Figure 5 DSC thermograms of PP and PP/FPP blends with different content of ATPU

Table 3 DSC data for PP and PP/FPP from heating scans

Content of ATPU(wt%)	T_{onset}(°C)	T_m(°C)	ΔT_m(°C)	ΔH_f(J/g)	X(%)
0	155.7	171.6	69.0	92.3	44.16
0.5	155.2	171.4	71.7	96.6	46.21
1.0	154.1	169.7	73.7	100.9	48.28
1.5	153.7	169.6	71.2	107.9	51.63
2.0	153.8	170.5	64.1	87.6	41.93
4.0	155.5	170.7	63.6	74.1	35.44

Table 4 DSC data for PP and PP/FPP from cooling scans

Content of ATPU(wt%)	T_{onset}(°C)	T_c(°C)	ΔT_c(°C)	ΔH_c(J/g)
0	112.6	108.7	46.2	97.3
0.5	117.1	112.3	39.7	103.5
1.0	118.3	113.4	33.7	104.8
1.5	118.8	114.5	34.8	113.7
2.0	120.7	117.2	39.2	105.8
4.0	120.7	116.8	33.2	88.1

enthalpy of 100% crystalline polymer(ΔH_0=209J/g). It turned out that the degree of crystallinity of PP/FPP was raised at a low content of ATPU (< 1.5wt%). However, further increasing the content of ATPU above 2.0wt% led to the reduction of the crystallinity. On other words, ATPU acted as a heterogeneous nucleating agent at low contents, which potentially increased the number of crystal grains in a unit volume. However, as the content of ATPU further increased, the effect of ATPU on heterogeneous nucleating was weakened, because there are too many crystal grains, for the available growth space. As a result, the spherocrystal growth of PP was restricted and the crystallinity was reduced. Therefore, ATPU plays a dual-role in crystallization of PP/FPP, either acting as a heterogeneous nucleating agent or an impurity. The former can improve crystallization, whereas the latter destroys the integrity of crystallization. The dual-functions of ATPU exist simultaneously. However, when the content of ATPU is below 2.0wt%, the nucleating effect is dominant, so that the crystallinity is raised. When the content of ATPU is above 2.0wt%, the structure integrity of samples tend to be spoiled and the capacity of crystallization declined.

For the samples containing ATPU, the crystallization onset temperatures(T_{onset}) are 5-8°C higher than that of PP homopolymer. T_c is 4-8°C higher than that of PP(108.7°C). Meanwhile, the ΔT_c is 7-12°C narrower than that of pure PP(46.2°C). The sample containing 4.0 wt% of ATPU led to higher T_c and minimum ΔT_c. The alternations in the crystallization enthalpies (ΔH_c) are related to the extent of crystallization. When the content of ATPU is lower than 2.0wt%, the values of ΔH_c for PP/FPP are always higher than that of pure PP and reaches the maximum at 1.5wt%. The results imply that the crystallization rate of blends was accelerated by functional groups at the level of 0.5-2.0wt%. The results were in accord with that obtained from isothermal crystallization analysis. The sample with 1.5wt% ATPU promoted PP crystallization most significantly since it showed the greatest ΔH_c among all modified samples and smaller ΔT_c. With the increase of ATPU content, the values of ΔH_c for PP/FPP decreased.

At the same time, we studied the PP/ ATPU blends with different contents of ATPU. Tables 5 and 6 present the results of DSC heating and cooling scans for the various blends.

Table 5 DSC data for PP and PP/ATPU from heating scans

Content of ATPU(wt%)	T_{onset}(°C)	T_m(°C)	ΔT_m(°C)	ΔH_f(J/g)	X(%)
0	155.8	171.6	69.0	92.29	44.16
0.5	154.7	170.0	68.9	82.38	39.42
1.0	154.9	172.6	66.7	83.72	40.06
1.5	154.2	170.6	66.1	82.43	39.44

Table 6 DSC data for PP and PP/ATPU from cooling scans

Content of ATPU(wt%)	T_{onset}(°C)	T_c(°C)	ΔT_c(°C)	ΔH_c(J/g)
0	112.6	108.7	46.2	97.32
0.5	117.4	112.3	37.0	93.32
1.0	117.4	112.8	40.8	96.12
1.5	117.9	112.8	39.7	96.00

As can be seen, the melting temperature (T_m) of the blends almost remains the same as that of PP, whereas the ΔH_f values of blends were lower than that of PP, indicating a decrease of crystallinity. Moreover, T_c of PP/ATPU blends was about 4°C higher than that of the PP, regardless of the various contents of ATPU in the blends. The crystallization behavior of PP/ATPU was also different from that of PP/PP-g-ATPU. In PP/PP-g-ATPU, ATPU was grafted on PP and well-dispersed in PP, leading to more crystal grains than those in PP/ATPU blends. As a result, PP-g-ATPU evidently accelerated the growth of crystallization.

Effect of FPP on the crystallinity and crystal parameters

PP is a polymorphic form material with a high tendency to crystallize, resulting in several crystal modifications[26], such as monoclinic(α), hexagonal(β), and triclinic(γ). Among them, α–modification is most frequently formed during PP, while β–modification often appears at a higher undercooling temperature. The γ–modification is observed in degraded, low molecular weight PP or when it crystallizes

under a high pressure. The WAXS diffractograms for PP and PP/FPP blends, shown in Figures 6, have similar features. The curves exhibit scattering angles at 2θ=14.100, 16.900, and 18.560, indicating an α-phase monoclinic structure. The degree of crystallinity can be estimated with the following formula:

$$Crystallinity(\%) = \frac{S_c}{S_c + S_a} \times 100 \tag{8}$$

where S_c is the area of crystallization and S_a is the amorphous area.

As can be seen in Figure 6, when the content of functional group is low in the samples (<1.5wt%), the crystallinity increased with an increase of functional group in the PP/FPP blends. The results are consistent with those found in DSC analysis.

The crystallite size (D) vertical to the lattice plane (hkl) can be obtained by Scherrer's equation:

$$D = \frac{k\lambda}{\beta \cos\theta} \tag{9}$$

where k is the factor of the crystal figure, λ is the wavelength of the X-ray(λ=1.541Å), and θ is the diffraction angle, β is equal to $(B^2 - b_0^2)^{1/2}$, where B is the width at half-tallness of the diffraction peak and b_0 is the broadening factor of the instrument, if we take no account of the lattice distortion, the equation can be simplified as follows:

$$D = \frac{0.89\lambda}{B \cos\theta}$$

The results of WAXS for PP and PP/FPP blends are shown in Table 7 and Figure 6, d_{hkl} is the space between lattice planes (hkl) and *I* is the relative intensity of crystalline peaks.

As can be seen, the crystallite size D decreased with an increasing amount of FPP. The D values for lattice planes 110 and 040 decrease more evidently than that of lattice plane 130. The results suggest that the crystallization of PP/FPP is less perfect than that of PP.

Table 7 Crystal Parameters of PP and PP/FPP Samples obtained from WAXS

Content of ATPU(wt%)	hkl	$2\theta/(°)$	d_{hkl}/nm	I	D/nm	X_c(%)
0	110	14.10	0.628	100	18.17	68.63
	040	16.90	0.524	44	20.91	
	130	18.56	0.478	32	20.37	
0.2	110	14.14	0.626	100	15.94	72.60
	040	16.92	0.524	64	20.70	
	130	18.58	0.477	45	17.43	
0.5	110	14.08	0.628	100	17.11	67.50
	040	16.88	0.525	65	20.49	
	130	18.56	0.478	39	20.85	
1.0	110	14.08	0.628	100	16.47	65.26
	040	16.86	0.525	70	20.59	
	130	18.56	0.478	41	19.20	

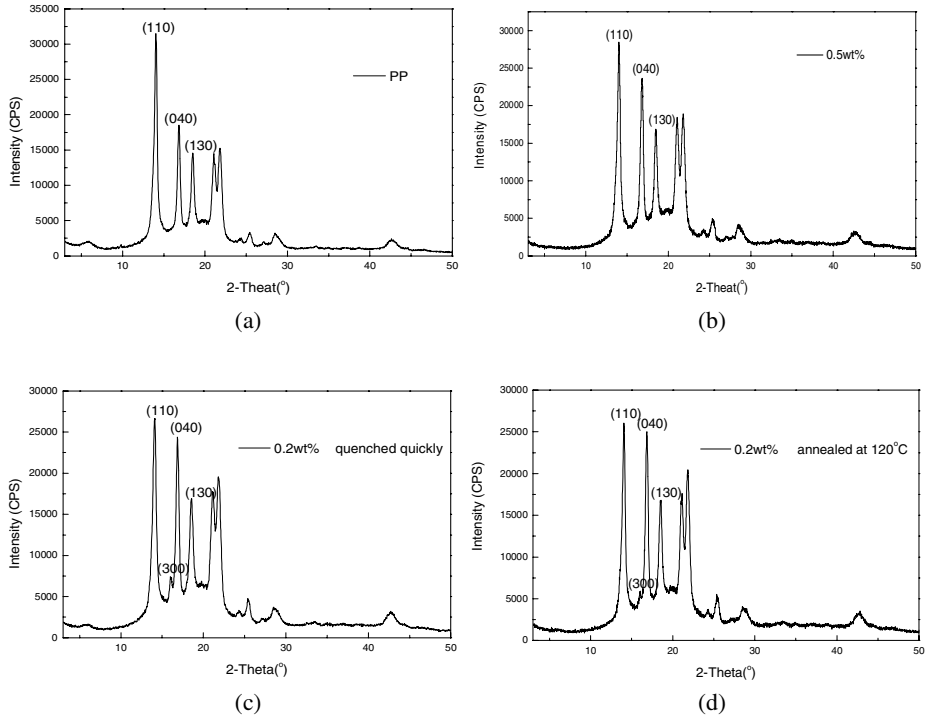

Figure 6 WAXS diffractogram of PP and PP/FPP blends:
(a) PP ; (b) 0.5wt%ATPU; (c) 0.2wt%ATPU quenched to room temperature quickly;
(d) 0.2wt%ATPU annealed at 120°C

Figure 6 (c) and (d) reveal the effect of cooling rate (quenched to room temperature and annealed at 120°C respectively). When the content of ATPU was low (<0.5wt%), β-phase hexagonal crystal was found in the modified PP. However, the structure disappeared as the content of ATPU increased. In spite of several advantages, such as higher impact strength, and good toughness, PP of β-crystalline form is not stable or readily transformable to the α-phase monoclinic structure under certain circumstances, such as the changes in temperature, temperature gradient and stress, etc.[27].

Morphological studies

Figure 7 shows polarized optical micrographs of PP and PP/FPP that were crystallized isothermally at 124°C. As can been seen inform Figure 7 (a), there are a number of spherulites impinging on each other for pure PP. The addition of FPP resulted in a decreased spherulite size but less perfection (Figure 7 (b) and (c)). At a high FPP content (2.0wt%) the spherulites were no longer clearly visible (Figure 7 (d)). The results indicated that spherulites size and perfection of PP crystal decreased as ATPU content increased, and were consistent with those obtained from DSC, WAXD and isothermal crystallization analysis.

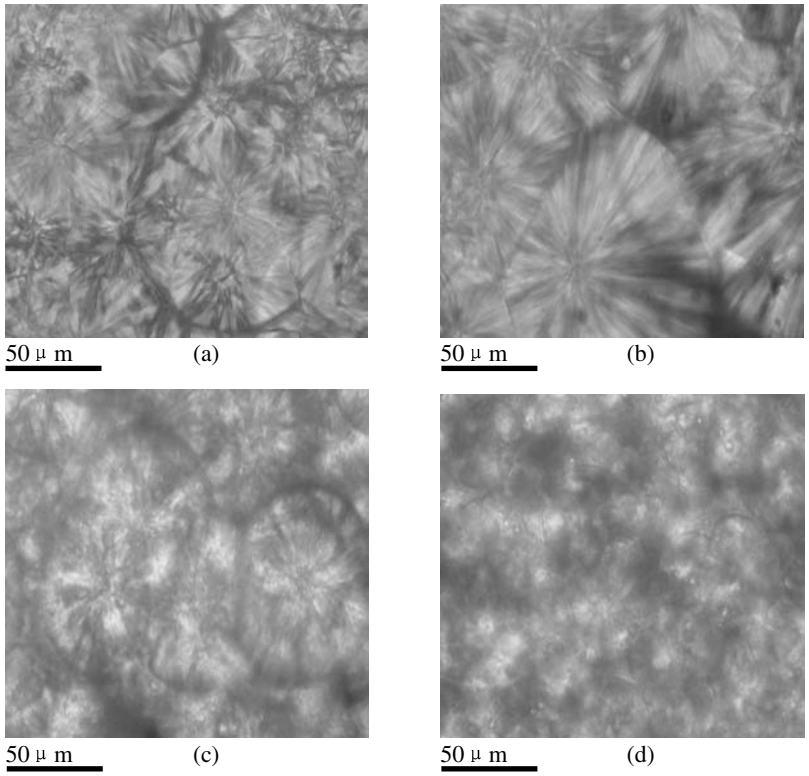

Figure 7 Polarized optical micrographs of PP and PP/FPP blends in isothermal crystallization at 124°C: (a) 0wt%ATPU; (b) 0.2wt% ATPU; (c)1.0wt% ATPU ; (d)2.0wt% ATPU

Conclusions

Blending FPP with PP did not alter the crystal conformation, but induced the formation of a small amount of β-phase crystal when the content of functional groups (i.e., ATPU) was less than 0.5wt%. When the content of FPP was low (below 2.0wt%), FPP acted as a heterogeneous nucleating agent and accelerated the crystallization. In an isothermal crystallization process, the crystallization rate of PP increased with the increase of FPP contents. When the content of ATPU was 2.0wt% or higher, the crystallinity decreased, and so did the crystallite sizes (D). It was found that the crystallization of the blends containing a high amount of ATPU was less perfect than that of PP homopolymer. The nucleation mode of PP/FPP blends was also more complicated than that of PP.

Acknowledgement The authors would like to acknowledge the financial support of the Shanghai Science Committee (No. 02dz11017).

Reference

[1] Ning P, Chen ZQ, Ren L,Huang T, Zeng FS.(2001) Journal of South China University of Technology (Natural Science Edition) 29:77.
[2] Avalos F, Lopez-Manchado MA. (1998) Arroyo M. Polymer39:6173.

[3] Arroyo M, Lopez-Manchado MA. (1997) Avalos F. Polymer 38:587.
[4] Lopez-Manchado M A, Arroyo M. (1999) Polymer 40:487.
[5] Bogoeva-Gaceva G, Janevski A, Mader E. (2001) Polymer 42:4409.
[6] Naga N, Mizunuma K, Sadatoshi H, Kakugo M. (2000) Polymer 41:203.
[7] Kobori Y, Akiba I, Akiyama S. (1999) Polym. Bull 43;285.
[8] Lo`pez Manchano MA, Biagiott J, Kenny JM. (2000) J Therm Anal Cal. 61:437.
[9] Arroyo M, Zitzumbo R, Avalos F. (2000) Polymer 41: 6351.
[10] Alwattari AA, Lloyd DR. (1998) Polymer 39:1129.
[11] Fan ZQ, Zhang YQ, Xu JT, Wang HT, Feng LX. (2001) Polymer 42: 5559.
[12] Kilwon Cho, Fengkui Li, Jaeseung Choi. (1999) Polymer 40:1719.
[13] Yu J, He J. (1999) Polymer 5:513.
[14] Ho RM, Su AC, Wu CH, Chen SL. (1993) Polymer 34:3264.
[15] Gayload NG, Mishra MK. (1983)J. Polym. Sci Polym Lett Ed. 21:23.
[16] Sun YJ, Hu GH, Lambla M. (1995) J.Appl. Polym. Sci. 57:1043.
[17] Yu J, He (2000) J. Polymer 41:891.
[18] Qi HJ, Yang XX.(1998) Journal of Qingdao University 13:1.
[19] Zhang XM, Wang DM. (1996) Polymer Material Science and Engineering 12:26.
[20] Yang XB, Zhan XL ,Chen FQ.(2003) Science Technology in Chemical Industry 11:20.
[21] Yin Zhihui, Zhang Yalie, Zhang Xiaomin, Yin Jinghua. (1997)J. Appl. Polym. Sci. 22:1565.
[22] Avrami M. (1939) J.Chem. Phys. 7:1103.
[23] Avrami M. (1940) J.Chem. Phys. 8:212.
[24] Chen Y, Xu M. (1998)Acta Polymerica Sinica 6:671.
[25] J. Pigłowski, I. Gancarz, M. Trelińska, H.W. Kammer, (2000) Polymer 41:6813.
[26] Gordana Bogoeva-gaceva, Aco Janevski, Anita Grozdanov.(1998) Journal of Applied Polymer Science 67:395.
[27] An F, Chen Y, Li BH. (2003) Synthetic Resin and Plastic 20:44.